ORIGINAL PAPER

Matthias Weiß · Robert Schöllhorn

Cathodic reduction of superconducting oxocuprates $YBa_2Cu_3O_{7-x}$ at high current densities

**Abstract** The cathodic reduction of $YBa_2Cu_3O_7$ in aqueous electrolytes at ambient temperature turns out to be strongly dependent upon current density with respect to the reaction mechanism. At low current density, topotactic electron/proton transfer is the dominant process, while at higher current densities, two competing reactions appear, i.e. the topotactic conversion and an irreversible reaction leading to products amorphous in terms of X-ray diffraction.

Key words Electron/proton transfer · Topotactic processes · Oxocuprates · High ionic strength electrolytes

Introduction

High temperature superconductors of the oxocuprate type have been the object of extended investigations for over a decade [1]. The physical and chemical properties of these compounds are intimately related to the presence of Cu^{2+}/Cu^{3+} mixed valence states. For $YBa_2Cu_3O_{7-x}$ the transition temperature T_c is correlated with the average valence of copper, which can be controlled by the oxygen stoichiometry in the range of $0 < x < 1$ via the oxygen partial pressure in the thermal synthesis procedure [2, 3] (Eq. 1):

$$YBa_2Cu_3O_7 \rightleftharpoons YBa_2Cu_3O_{7-x} + (x/2)O_2 \qquad (1)$$
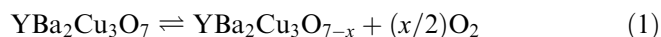
Soon after the discovery of the superconducting properties of $YBa_2Cu_3O_{7-x}$, attempts were made to modify the copper valence and thus the superconducting transition temperature at *low* temperatures by electrochemical electron/ion transfer reactions which should give access via kinetic control to metastable phases not accessible via thermal processes. The results of these early investigations were characterized, however, by the appearance of side reactions leading to partial irreversible decomposition in aqueous electrolytes [4]. A considerable number of studies were restricted to fast cyclovoltammetry, i.e. to surface processes [5–13]. Some investigations were performed also in nonaqueous electrolytes, focusing on the intercalation of lithium ions [14–16]. A review of the research activities on the electrochemistry of high-T_c superconductors to the middle of the current decade is given by McDevitt et al. [17].

Recently we reported on new results concerning the topotactic cathodic reduction of $YBa_2Cu_3O_7$ in aqueous electrolytes at ambient temperature [18]. We were able to demonstrate that the corrosion problems in earlier studies were associated with the electrolyte. The use of high ionic strength electrolytes allowed for the first time quantitative electrochemical reduction without decomposition reactions. It could be shown that the terminal reduction product corresponds to that obtained by the reaction of hydrogen with $YBa_2Cu_3O_7$ at 100–200 °C [19, 20]; the reduction can be described as an electron/proton transfer process (Eq. 2):

$$xH^+ + xe^- + YBa_2Cu_3O_7 \rightarrow YBa_2Cu_3O_{7-x}OH_x \qquad (2)$$
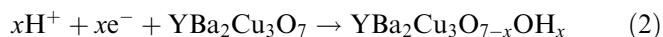
The electrochemical reaction starts with a one-phase region ($0 < x < {\sim}0.2$, A2 phase). The subsequent two-phase region leads to the terminal product with a charge transfer of 0.66 e^-/f.u. $YBa_2Cu_3O_7$ (A1 phase).

The aim of the present study was the understanding of significant changes in the reaction process observed when the cathodic reduction of $YBa_2Cu_3O_7$ was performed at elevated current densities.

Experimental

Reagents used were of analytical grade purity. The preparation of the $YBa_2Cu_3O_7$ samples was performed via the conventional solid state technique with Y_2O_3, $BaCO_3$ and CuO as the educts (sintering at 940 °C, repeated grinding, annealing at 400 °C; 1 bar oxygen

M. Weiß · R. Schöllhorn (✉)
Technische Universität Berlin,
Institut für Anorganische und
Analytische Chemie, Strasse des 17 Juni 135,
10623 Berlin, Germany

atmosphere). Samples with maximal oxygen stoichiometry had a composition equivalent to $YBa_2Cu_3O_{6.94}$; in the general discussion and in equations, "$YBa_2Cu_3O_7$" is used to designate this phase for simplicity reasons. Samples with lower oxygen stoichiometry were obtained by heating $YBa_2Cu_3O_{6.94}$ to defined temperatures with subsequent quenching in liquid nitrogen. The following reheating to room temperature occurred under vacuum in order to avoid corrosion by water vapor condensation.

The oxidation state of Cu in all samples was determined by iodometric titration, which also served for the calculation of the oxygen content of sintered $YBa_2Cu_3O_{7-x}$ samples [21, 22]. Powder X-ray diffraction measurements were carried out in reflection mode with a Siemens D 5000 instrument in Bragg-Brentano geometry with a position sensitive detector and Cu K_α radiation.

The electrochemical standard experiments were performed at 300 K in cells with a conventional three-electrode arrangement. The working electrode consisted of cylindrical sintered samples (diameter 10 mm, thickness 0.3–1 mm) mechanically contacted by platinum clamps. The reference electrode was a Ag/AgCl unit filled with 3 M aqueous KCl solution. Commercial equipment was used for electrochemical experiments in galvanostatic or voltammetric mode. Saturated aqueous $LiNO_3$ solution (8.2 M) served as standard electrolyte.

Since the dimensions of the cylindrical working electrode pellets were kept approximately constant, the nominal current density is given in the following as the current/electrode mass ratio, µA/mg.

Results and discussion

A typical potential/charge transfer curve for the galvanostatic cathodic reduction of $YBa_2Cu_3O_{6.94}$ under standard conditions ($I \leq 0.4$ µA/mg, saturated aqueous $LiNO_3$ electrolyte) is given as graph 1 in Fig. 1 [18]. After the initial one-phase region (phase A2) a potential plateau is observed at ca. 100 mV corresponding to a two-phase region (A2/A1) with A1 as the terminal reaction product. The characteristic reaction time until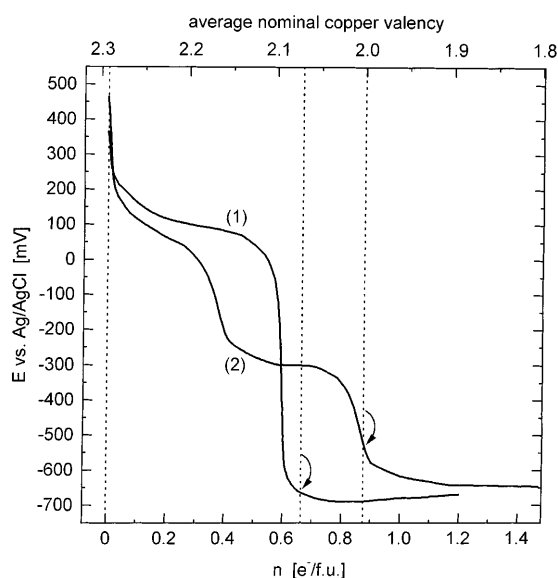 the potential of electrolyte decomposition (−600 to −700 mV) is reached corresponds to ca. 3 days. The degree of reduction obtained nominally at the end point of the electrochemical reaction (Eq. 2) is indicated by an arrow and agrees with the iodometric values.

If current densities > 0.8 µA/mg are applied under otherwise identical standard conditions the potential/charge transfer curve changes significantly; a typical curve is shown in Fig. 1, graph 2. The potential in the initial region is now more negative and a new potential plateau at ca. −300 mV appears. The nominal charge transfer as determined by iodometric titration was 0.88 e⁻/f.u. and thus is significantly higher compared to low current density conditions. This seems to be unusual since in normal electrochemical reactions higher current densities lead to lower yields, related to the nominal charge transfer and a loss of structural information compared to the galvanostatic equilibrium curve for kinetic reasons. The newly appearing potential plateau at −300 mV suggests that the reaction process at higher current densities is different from that at low current densities.

Characteristic sections of X-ray powder diagrams of products obtained with low and high current densities but otherwise identical conditions are given in Fig. 2. Both diagrams exhibit changes relative to the educt phase characteristic for the conversion to A1, i.e. a peak shift of the 001 reflection corresponding to a c-axis change of 6%, a strong decrease in line intensity of all other c-axis dominated reflections and an increased line width [18]. These characteristics appear less pronounced, however, for the product obtained at high current density, although the nominal conversion in terms of iodometric titration is larger. Under these aspects a further shift of the 001 reflection to lower angle values is to be expected, but is not observed, however. The product obtained at high current densities with considerably
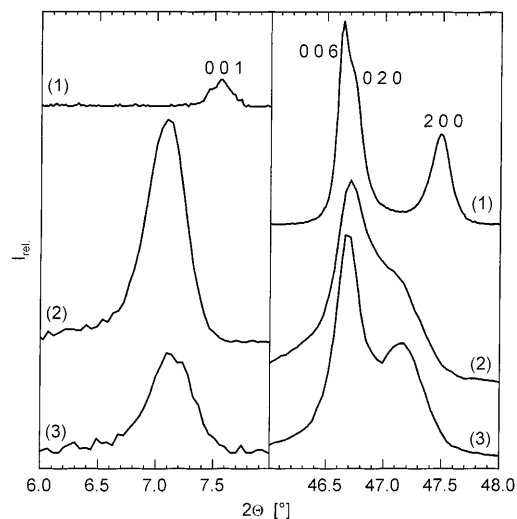

Fig. 1 Potential/charge transfer curves for the galvanostatic cathodic reduction of $YBa_2Cu_3O_{6.94}$ under standard conditions; *1* low current density ($I \leq 0.4$ µA/mg) [18]; *2* high current density ($I > 0.8$ µA/mg)

Fig. 2 Selected sections of X-ray powder diagrams: *1* educt $YBa_2Cu_3O_{6.94}$; *2* reaction product obtained at low current density; *3* reaction product obtained at high current density

larger nominal conversion does obviously not lead to a reduction beyond phase A1 to subsequent phases A and B which have been identified earlier by chemical reduction with H_2 at higher temperatures [19, 20].

In order to characterize these differences, galvanostatic reductions were performed at high current densities and interrupted after defined charge transfer values. The X-ray diffractograms of the products exhibited, however, a lack of reproducibility in structural terms at constant reaction conditions; similarly, the curve shapes were not reproducible with satisfying accuracy. It was found that the maximum extent of reduction as determined by iodometry was increasing with increasing length of the potential plateau at −300 mV. The galvanostatic experiments showed furthermore that the earlier this plateau was reached the more extended it appeared.

For comparison reasons, further experiments were carried out by slow scanning voltammetry (SSV) with voltage scan rates of 40–80 mV/h in order to reach quantitative conversion of the electrode material. The current densities observed under these conditions were significantly higher compared to those applied in galvanostatic experiments. No cycling was used since the electrode environment became strongly acidic upon oxidation, which favored decomposition processes.

In Fig. 3, examples for voltammetric reduction curves for $YBa_2Cu_3O_{6.94}$ are shown with a scan rate of 75 mV/h. The upper curve 1 was obtained with standard aqueous $LiNO_3$ electrolyte. Two reduction peaks are clearly visible with maxima at 0 mV and −400 mV. These potentials correspond reasonably well with those observed on fast galvanostatic reduction. The potential shift for about 100 mV to the negative region is due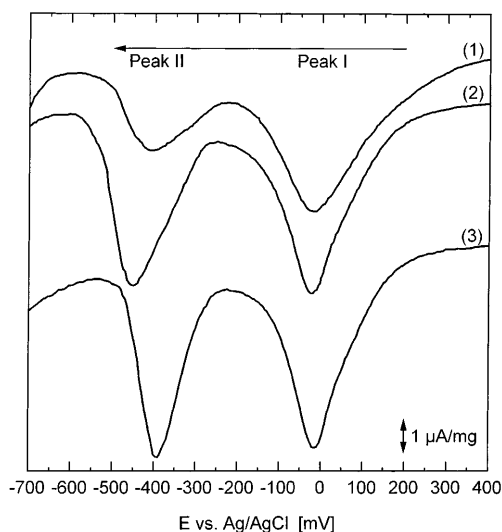 to the strongly increased current densities compared to galvanostatic experiments. In the following text we will describe the voltammetric peak at higher potential as peak I and the one at lower potential as peak II.

Sections of X-ray diffractograms from samples obtained upon interruption of the reaction after peak I and after peak II are given in Fig. 4. They confirm that the standard product phase A1 is clearly present already after the completion of peak I; no starting material can be detected at this point. However, the shoulder on the 001 reflection of the A1 phase (Fig. 4, curve 2) indicates the presence of the protonated phase A2. It is concluded that upon fast cathodic reduction the reaction starts with the formation of the phase A2; simultaneously, however, the reduction to A1 proceeds so that at the end of the first voltammetric peak the majority phase is already A1. At the end of the second cycle only phase A1 can be detected by X-ray diffraction.

In order to investigate a potential influence of the electrolyte alkali cation on the reaction process, saturated aqueous solutions of $LiNO_3$, $NaNO_3$ and KNO_3 were compared in voltammetric mode. The curves obtained are essentially identical (Fig. 3); the same is true for the X-ray data of the products obtained after the first and second peak. It can be concluded thus that the electrolyte cation does not affect the voltammetric reaction; it was proved earlier that under standard galvanostatic conditions no influence of the alkali cation type is found [18]. Similar results were reported in cyclovoltammetric studies with scan rates ca. 400 times higher than those used here in alkali hydroxide electrolytes [9]. In all cases the cathodic section was found to exhibit two peaks.

The *concentration* of the electrolyte was found, however, to exert a clear influence on the cathodic reduction of $YBa_2Cu_3O_{6.94}$ at ambient temperature. Figure 5 shows the SSV curves with a rather low scan
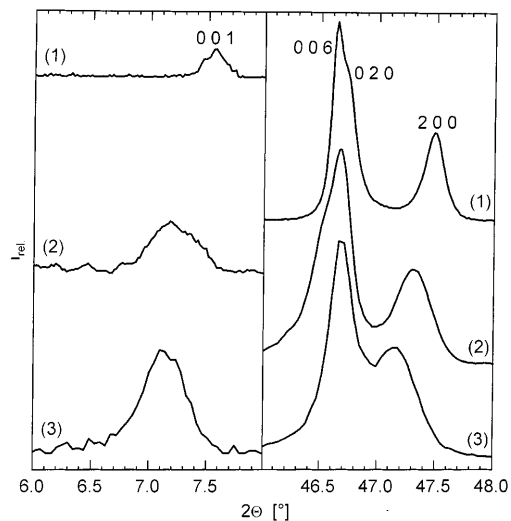

Fig. 3 Slow scanning voltammetry (SSV) with $YBa_2Cu_3O_{6.94}$ working electrodes; voltage scan rate 75 mV/h; *1* standard electrolyte of saturated aqueous $LiNO_3$ (8.2 M); *2* saturated aqueous $NaNO_3$ (10.5 M); *3* saturated aqueous KNO_3 (3.1 M)

Fig. 4 Sections of X-ray powder diffractograms: *1* educt $YBa_2Cu_3O_{6.94}$; *2* product obtained after passage of peak I; *3* product after passage of peak II
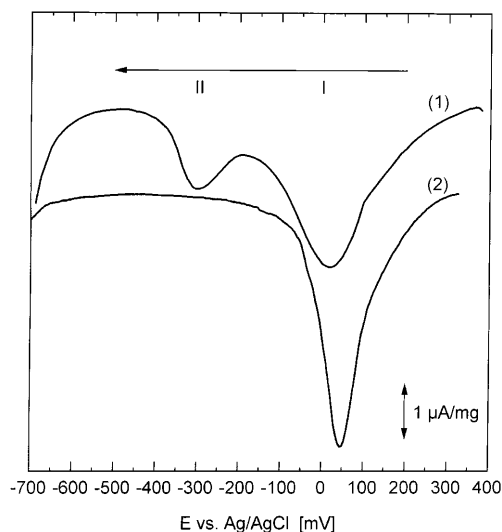
Fig. 5 SSV (voltage scan rate 42 mV/h) with $YBa_2Cu_3O_{6.94}$ working electrodes: *1* saturated aqueous $LiNO_3$ electrolyte (8.2 M); *2* 1 M aqueous $LiNO_3$

rate of 42 mV/h for aqueous $LiNO_3$ electrolyte with different concentrations. Curve 2 demonstrates that at low $LiNO_3$ concentration (1 M) the peak at lower potential is clearly absent. This means that the voltammetric reduction at low electrolyte concentration proceeds similar to the galvanostatic reduction at low current densities. The disadvantage of the use of lower salt concentration, as proved earlier in galvanostatic experiments, is considerable corrosion under release of Ba^{2+} ions [18].

The application of lower voltage scan rates was found to have a similar influence on the voltammetric reaction as the reduction of the electrolyte concentration. Figure 6 displays the reduction process in saturated aqueous KNO_3 solution. At a scan rate of 75 mV/h the two peak
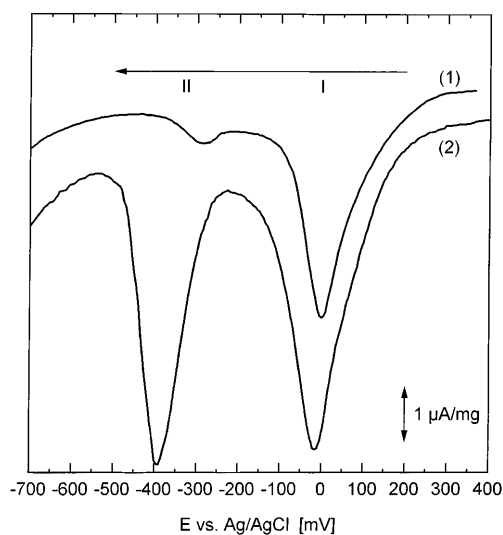
areas are approximately equivalent, while at a 40% reduced scan rate the reduction peak II exhibits a substantially smaller area. The intensity of peak II thus increases strongly with the scan rate, i.e. the reaction kinetics.

It is obvious that the reaction process in voltammetric reduction displays correlations with electrolyte concentration and with scan rate. Upon decreasing electrolyte concentration the scan rate must be increased in order to achieve a two-step reduction. Inversely, the reduction process can be carried out either as a two-step or as a one-step reaction at any electrolyte concentration, if the scan rate is appropriately selected.

The correlations described above concern the reduction of $YBa_2Cu_3O_{6.94}$, i.e. the phase with maximum oxygen content that can be prepared at 1 bar O_2. The investigation of samples with lower oxygen stoichiometry, $YBa_2Cu_3O_{7-x}$ ($x > 0.06$), demonstrates that there is no influence in this case of the electrolyte concentration on the reaction process. Increasing scan rate (voltammetry) or current density (galvanostatic mode) was found to lead to increasing decomposition of the working electrode.

Figure 7 illustrates characteristic voltammetric curves for the reduction of $YBa_2Cu_3O_{7-x}$ samples with varying oxygen stoichiometry in saturated aqueous $LiNO_3$ electrolyte with a constant scan rate of 43 mV/h. It can be seen that the appearance of the reduction peak I is directly related to the oxygen stoichiometry of the educt. For samples with an average copper oxidation state $< +2$ (i.e. no nominal Cu^{3+} content), peak I is absent (Fig. 7, curve 3 for $YBa_2Cu_3O_{6.41}$). The second reduction peak always appears, independent of the educt oxygen stoichiometry. It can thus be assumed that the first reduction peak is formally associated with the reduction of Cu^{3+} to Cu^{2+}. Earlier cyclovoltammetric studies in

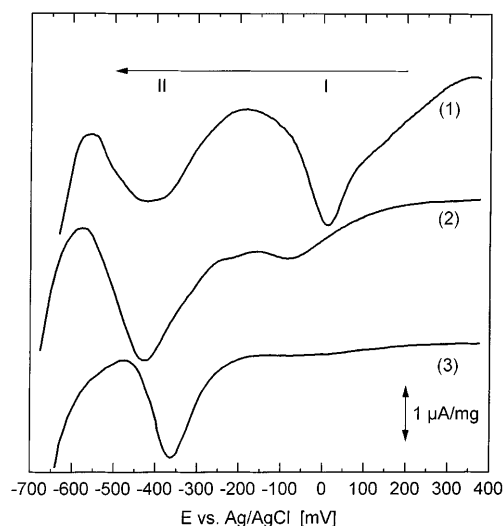**Fig. 6** SSV with $YBa_2Cu_3O_{6.94}$ in saturated aqueous KNO_3 electrolyte (3.1 M); *1* potential scan rate 44 mV/h; *2* 75 mV/h

Fig. 7 SSV (43 mV/h) in saturated aqueous $LiNO_3$ electrolyte with the working electrodes: *1* $YBa_2Cu_3O_{6.94}$; *2* $YBa_2Cu_3O_{6.69}$; *3* $YBa_2Cu_3O_{6.41}$

alkali hydroxide electrolytes came to a similar conclusion [9]. The authors relate the first and second reduction peak to the conversion $Cu^{3+} \rightarrow Cu^{2+}$ and $Cu^{2+} \rightarrow Cu^{+}$, respectively, without a discussion of appearing real phases. The structural changes reported here suggest, however, that in terms of chemical phases and mechanism, quite different processes are associated with the two reduction peaks.

In Fig. 8, characteristic sections of X-ray diffractograms are given for $YBa_2Cu_3O_{6.69}$ and of the product obtained after complete voltammetric cathodic reduction (end of peak II). The corresponding voltammetric curve is illustrated in Fig. 7, graph 2. The X-ray data show that only a partial conversion to the product phase A1 takes place; the 001 reflection of the educt phase is still clearly visible. This relates well with the corresponding voltammetric curve: the first reduction peak – which is responsible for the conversion to A1 according to the results discussed above – is rather weak only. The major conversion has to be attributed to peak II without visible consequence for the product diffractogram, however. This aspect is even more clearly demonstrated when the voltammetric reduction of $YBa_2Cu_3O_{6.41}$ is considered, as illustrated in curve 3 of Fig. 7. We can find here only the second reduction peak and, as expected, no differences in the X-ray diffractograms of educt and product are observed (Fig. 9).

The experimental results presented above can be interpreted in terms of a coherent model for the cathodic reduction of $YBa_2Cu_3O_{7-x}$ at *high* current density, i.e. fast reaction kinetics. Under these conditions the reaction proceeds in two steps. In the first step, at higher potential, the topotactic electron/proton transfer starts with the formation of the nonstoichiometric phase A2, while simultaneously the transformation to the product phase A1 occurs, i.e. nonequilibrium conditions. This
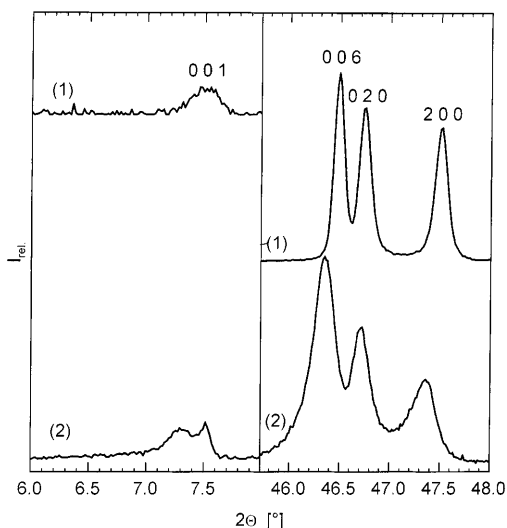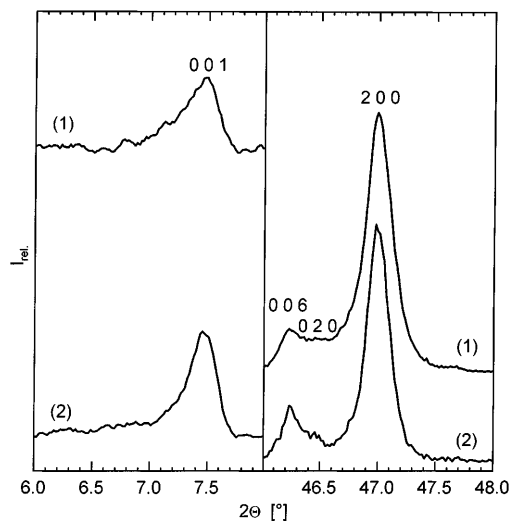

Fig. 9 Sections of X-ray powder diffractograms: *1* $YBa_2Cu_3O_{6.41}$; *2* product after complete reduction (Fig. 7, graph 3)

conversion is correlated with defined structural changes as demonstrated by the X-ray diffractograms. Under standard conditions with *low* current density and quasiequilibrium conditions the charge transfer maximum is equivalent to 0.66 e^-/f.u. [18]; this value decreases with increasing current densities above 0.4 μA/mg. In addition, the charge transfer obtained in the first step is dependent upon the oxygen stoichiometry of the educt. It can be assumed that the topotactic process corresponds formally to a reduction of Cu^{3+} in the solid by electron/proton transfer, i.e. this reaction is possible only as long as Cu^{3+} ions are present in the educt.

The second step at high current densities at the more negative potential does not represent a topotactic process. This is demonstrated by the fact that the X-ray diffractograms remain unchanged under conditions which allow reaction only in this potential region (absence of peak I). In analytical terms (iodometric titration), however, it can be proved that the chemical reduction continues like in the first step. Our conclusion is therefore that in the second step (1) no topotactic process takes place and (2) the products are *amorphous* in terms of X-ray diffraction. The products obtained after the second step therefore represent – dependent upon the current density – mixtures of amorphous decomposition phases with A1 (Fig. 10). The topotactic electron/proton transfer of the first step and the irreversible decomposition of the second step are then competing reactions, provided the oxidation state of the educt is high enough to admit the topotactic process. This is confirmed by the scan rate dependence of the intensity of the second step in voltammetric reductions of $YBa_2Cu_3O_{6.94}$ and by the correlation between the beginning and extension of the potential plateau in galvanostatic reactions. In both cases, the lower the extent to which the sample is converted to A1 in the first step, then the higher is the conversion extent in the second step.

Fig. 8 Sections of X-ray powder diffractograms: *1* $YBa_2Cu_3O_{6.69}$; *2* product obtained after peak II, i.e. complete voltammetric reduction (Fig. 7, graph 2)

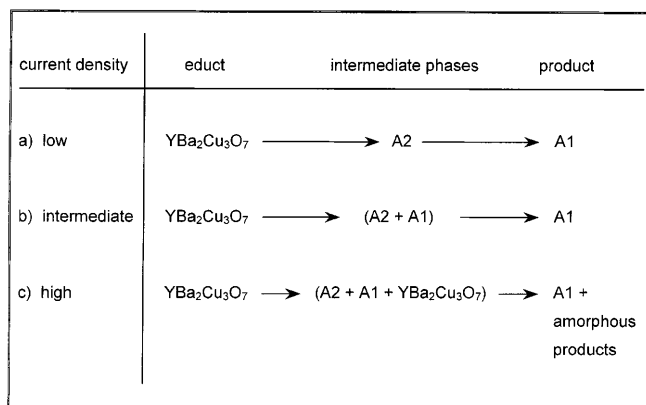| current density	educt	intermediate phases	product
a) low	$YBa_2Cu_3O_7$ ⟶	$A2$ ⟶	$A1$
b) intermediate	$YBa_2Cu_3O_7$ ⟶	$(A2 + A1)$ ⟶	$A1$
c) high	$YBa_2Cu_3O_7$ ⟶	$(A2 + A1 + YBa_2Cu_3O_7)$ ⟶	$A1$ + amorphous products

Fig. 10 Scheme for the cathodic reduction of $YBa_2Cu_3O_7$ at different current densities: *a* quasi-equilibrium process with the sequential formation of intermediates and terminal product; *b, c* strong influence of kinetics, nonequilibrium systems with simultaneous formation of intermediates, terminal product and phases from irreversible decomposition

The second step at lower potential is independent of the average nominal Cu valence in the educt, i.e. this reaction proceeds also with samples that do not contain Cu^{3+}. As proposed earlier on grounds of cyclovoltammetric studies, this step can be formally associated with the reduction of Cu^{2+} to Cu^+. We have no information on the reaction mechanism, however, since the products formed in this step are amorphous to X-rays according to the present investigations. It is clear, however, that it is not a topotactic process.

The observed dependence of the second reaction step upon the electrolyte concentration demonstrates the difference between the reductive decomposition to amorphous products and the normal corrosion reactions in aqueous electrolytes which are due to acid/base reactions. The second step in the cathodic reduction appears to be kinetically restrained in dilute electrolytes (high current densities required); the corrosive acid/base type decomposition is favored under these conditions.

Conclusions

It is the combination of two different modes of electrochemical reduction combined with the investigation of structural changes that allowed a successful analysis of the difference in reactivity observed upon cathodic reduction of $YBa_2Cu_3O_7$ at ambient temperature in aqueous electrolytes at low and at high current densities. It is obvious that kinetics are strongly influencing the complex mechanisms. In agreement with earlier studies [4, 18, 23–25], the message is again that oxocuprate-type phases are highly reactive systems at room temperature with respect to acid/base as well as redox reactions.

References

1. Schöllhorn R (1988) Angew Chem 100: 1446; Angew Chem Int Ed Engl 27: 1392
2. Krüger Ch, Conder K, Schwer H, Kaldis E (1997) J Solid State Chem 134: 356
3. Jorgensen JD, Veal BW, Paulikas AP, Nowicki LJ, Crabtree GW, Claus H, Kwok WK (1990) Phys Rev B 41: 1863
4. Eickenbusch H, Paulus W, Gocke E, March JF, Koch H, Schöllhorn R (1987) Angew Chem 99: 1201; Angew Chem Int Ed Engl 26: 1188
5. Bachtler H, Lorenz WJ, Schindler W, Saemann-Ischenko G (1988) J Electrochem Soc 135: 2284
6. Rosamilia JM, Miller B (1988) J Electroanal Chem 249: 205
7. Rochiani S, Hibbert DB, Dou SX, Bourdillon AJ, Liu HK, Zhou JP, Sorrell CC (1988) J Electroanal Chem 248: 461
8. Rosamilia JM, Miller B (1989) Anal Chem 61: 1497
9. Barsch U, Beck F (1990) Electrochim Acta 35: 759
10. Beck F, Barsch U (1990) J Electroanal Chem 282: 175
11. San José MT, Espinosa AM, Tascón ML, Vázquez MD, Batanero PS (1991) Electochim Acta 36: 1209
12. Hepburn BJ, Lau HL, Lyon SB, Newman RC, Thompson GE, Alford N (1992) Corros Sci 33: 515
13. Scheurell S, Scholz F, Olesch T, Kemnitz E (1992) Supercond Sci Technol 5: 303
14. Vondrák J, Jakubec I, Bludská J, Skácel V (1990) Electrochim Acta 35: 995
15. Fleischer NA, Lyubomirsky I, Scolnik Y, Manassen J (1993) Solid State Ionics 59: 59
16. Molenda J, Bak T, Stoklosa A (1993) Physica C 207: 147
17. McDevitt JT, Haupt SG, Jones CE (1996) Electrochemistry of high-T_c superconductors. In: Bard AJ, Rubinstein I (eds) electroanalytical chemistry, vol 19. Dekker, New York, pp 337–486
18. Weiß M, Günther W, Schöllhorn R (1998) Physica C 304: 156
19. Günther W, Schöllhorn R (1997) Solid State Ionics 101–103: 1335
20. Günther W, Schöllhorn R, Epple M, Siegle H, Thomsen C, Kabius B, Poppe U, Schubert J, Zander W (1999) Philos Mag A 79: 449
21. Lanza P, Rossi G (1991) Anal Chim Acta 244: 253
22. Weiß M (1998) Dissertation. Technische Universität Berlin
23. Wattiaux A, Park JC, Grenier JC, Pouchard M (1990) C R Acad Sci Paris Ser II 310: 1047
24. Rudolf P, Paulus W, Schöllhorn R (1991) Adv Mater 3: 438
25. Rudolf P, Schöllhorn R (1992) J Chem Soc Chem Commun 1158